MAGNETIC PROPERTIES OF ANTIFERROMAGNETICALLY ORDERED KRAMERS LIGHT RARE-EARTH COMPOUNDS. PART II

By P. Szweykowski

Institute of Physics, A. Mickiewicz University, Poznań*

(Received May 14, 1977)

The role of combined crystal field and exchange effects in the magnetic properties of Kramers light rare-earth compounds is studied. Results are obtained in the molecular-field approximation including an external field directed along the magnetic order. As an example, cerium compounds having a cubic crystal structure with tetragonal distortion are considered. The conclusions cover a wide range of the molecular field/crystal field ratio. The importance of the crystal field in determining the magnetic behaviour is clearly demonstrated.

1. The molecular-field Hamiltonian

Within the framework of our simplified model, we assume the antiferromagnetic collinear ordering along the (001) crystal axis of the cubic structure (see, for example, [1–9]). Below the Néel temperature, Ce^{+3} ions form two interpenetrating magnetic sublattices and all the nearest neighbours of an ion belong to the other sublattice (see, [10]). The Hamiltonian of such a system can be written as follows:

$$\hat{H} = \sum_l \hat{H}_{cf}(l) - \sum_{l,m} J_{lm}(\hat{\vec{J}}_l, \hat{\vec{J}}_m), \tag{1}$$

where $\hat{H}_{cf}(l)$ is the single-ion crystal-field Hamiltonian; summation in the second term comprises all the nearest-neighbour pairs and the bilinear exchange parameter J_{lm} is assumed to be negative to ensure antiferromagnetic coupling.

In order to obtain the molecular-field Hamiltonian, we perform the well-known transformation (see: for example, [10] and Refs therein):

$$\hat{\vec{J}}_l = \hat{\vec{j}}_l + \langle \hat{J}_l^z \rangle \vec{\sigma}_z \tag{2}$$

where $\vec{\sigma}_z$ is the unit vector in the direction of the magnetic ordering, and $\langle \hat{J}_l^z \rangle$ the canonical thermal average of the operator of the z-component of total angular momentum. The

* Address: Instytut Fizyki, Uniwersytet im. A. Mickiewicza, Matejki 48/49, 60-769 Poznań, Poland.

term $-\sum_{l,m} J_{lm}(\hat{\vec{J}}_l, \hat{\vec{J}}_m)$ gives rise to magnetic collective excitations and is neglected within the framework of the molecular-field approximation (cf also [10, 13, 14]).

Having taken into account the occurrence of the two magnetic sublattices (A and B) with N ions on each sublattice, we arrive at the effective field Hamiltonian in the following form:

$$\hat{H}_{\mathrm{mf}} = \sum_{l\in A} [\hat{H}_{\mathrm{cf}}(l) - \mathscr{H}^{A}_{\mathrm{mf}} \hat{J}^z_l] + \sum_{m\in B} [\hat{H}_{\mathrm{cf}}(m) - \mathscr{H}^{B}_{\mathrm{mf}} \hat{J}^z_m] + NJ(0) \langle \hat{J}^z_A \rangle \langle \hat{J}^z_B \rangle, \tag{3}$$

where $\mathscr{H}^{A(B)}_{\mathrm{mf}}$ is the molecular-field strength, expressed in unit of energy, $\langle \hat{J}^z_A \rangle$ and $\langle \hat{J}^z_B \rangle$ are the thermal averages of the operator $\hat{J}^z$ at a site belonging to the sublattice A and B, respectively. $J(0)$ is the Fourier transform of the exchange interaction for the reciprocal vector equal to zero: $J(\vec{k}) = \sum_m \exp[i(\vec{k}, \vec{R}_m)] J_{lm}$.

Obviously, in our simplified model, the following relation holds:

$$\mathscr{H}^{A(B)}_{\mathrm{mf}} = \lambda_{\mathrm{af}} \langle \hat{J}^z_{A(B)} \rangle, \tag{4}$$

where λ_{af} is the antiferromagnetic molecular-field constant, expressed in units of energy. In order to study the influence of an external field applied along the magnetic direction, we introduce the appropriate Zeeman term into the Hamiltonian (3) ([1, 2])

$$\hat{H}_z = -H_z(1+\lambda_{\mathrm{p}}\chi_{\|}) \sum_i \hat{J}^z_i, \tag{5}$$

where H_z is the external field strength in units of energy, $\chi_{\|}$ the longitudinal magnetic susceptibility, λ_{p} the paramagnetic molecular field constant, and $\lambda_{\mathrm{p}} X_{\|} H_z$ is an extra field acting on each ion due to its exchange coupling to the other ions, at which the external magnetic field induces an additional moment $\chi_{\|} H_z$.

The total Hamiltonian of a single ion now takes the following form:

$$\hat{H}(l) = \hat{H}_{\mathrm{mf}}(l) + \hat{H}_z(l), \tag{6}$$

where we have denoted

$$\hat{H}_z(l) = -H_z(1+\lambda_{\mathrm{p}}\chi_{\|}) \hat{J}^z_l \tag{6a}$$

and the Hamiltonian $H_{\mathrm{mp}}(l)$ comprises the crystal-field term also (cf. Eq. (3)).

The Hamiltonian $\hat{H}(l)$ is diagonalized in the basis of crystal-field eigen-states (for the details see, for example, [2, 3, 5, 13]). The simple procedure yields six energy values and six corresponding wave functions. We can now use them to derive the thermal averages of selected magnetic quantities.

2. Derivation of the magnetic quantities

We concentrate our discussion on the behaviour of the following quantities:

(*i*) the sublattice magnetization per ion $\langle \hat{J}^z_A \rangle$ and $\langle \hat{J}^z_B \rangle$ together with the total magnetization per ion: $m = \frac{1}{2}(\langle \hat{J}^z_A \rangle + \langle \hat{J}^z_B \rangle)$ and the difference between the sublattice magnetiza-

tions defined as $\varepsilon = \frac{1}{2}(\langle \hat{J}_A^z \rangle - \langle \hat{J}_B^z \rangle)$ these quantities being expressed in units of $g\mu_B$, g — Landé's factor, μ_B — Bohr's magneton;

(*ii*) the longitudinal susceptibility $\chi_{\|}$

(*iii*) the magnetic specific heat C_H.

Below the Néel temperature the sublattice magnetizations at zero external field can be obtained from the following self-consistent equations:

$$\langle J_{A(B)}^z \rangle = \frac{1}{Z_{A(B)}} \sum_{l=1}^{6} \langle \Gamma_i^{A(B)}, J^z \Gamma_i^{A(B)} \rangle e^{-E_{\Gamma i}^{A(B)}/\theta}, \tag{7}$$

where $E_{\Gamma_i}^{A(B)}$ and $|\Gamma_i^{A(B)}\rangle$ are six eigen-values and eigen-states of the Hamiltonian $\hat{H}(l)$ with H_z put equal to zero for l belonging to the sublattice A and B, respectively; and $\theta = kT^{-1}$. Obviously, without a field, we have $m = 0$ and $\varepsilon = \langle J_A^z \rangle$ in the ordered régime, whereas above the Néel temperature all four quantities vanish. Derivation of the external field-dependence of the magnetizations requires that the longitudinal susceptibility of the system shall be available. The longitudinal susceptibility is calculated from the following self-consistent equation (cf. [10]):

$$\chi_{\|} = \frac{\frac{1}{2}(\chi_A^0 + \chi_B^0)}{1 - \frac{1}{2}\lambda_{af}(\chi_A^0 + \chi_B^0)}, \tag{8}$$

where χ_A^0 and χ_B^0 are defined as the sublattice longitudinal susceptibilities by the formula:

$$\chi_{A(B)}^0 = \frac{\partial \langle J_{A(B)}^z \rangle}{\partial H_z}. \tag{8a}$$

Explicitly, the equation for χ_A^0 or χ_B^0 can be written as follows (Eq. (4a) of Part I):

$$\begin{aligned} \chi_{A(B)}^0 = {} & \frac{1}{\theta} \frac{1}{Z_{A(B)}} \sum_{\substack{i,j=1 \\ (E_{\Gamma i} = E_{\Gamma j})}}^{6} \langle \Gamma_i^{A(B)}, J^z \Gamma_j^{A(B)} \rangle^2 \exp(-E_{\Gamma i}^{A(B)}/\theta) \\ & - \frac{1}{\theta} \left\{ \frac{1}{Z_{A(B)}} \sum_{\substack{i,j=1 \\ (E_{\Gamma i} = E_{\Gamma})}}^{6} \langle \Gamma_i^{A(B)}, J^z \Gamma_j^{A(B)} \rangle \exp(-E_{\Gamma_i}^{A(B)}/\theta) \right\}^2 \\ & + \frac{2}{Z_{A(B)}} \sum_{\substack{i,j=1 \\ (E_{\Gamma i} \neq E_{\Gamma j})}}^{6} \frac{|\langle \Gamma_i^{A(B)}, J^z \Gamma_j^{A(B)} \rangle|^2}{E_{\Gamma_i}^{A(B)} - E_{\Gamma_j}^{A(B)}} \exp(-E_{\Gamma_j}^{A(B)}/\theta) \end{aligned} \tag{8b}$$

where $E_{\Gamma_i}^{A(B)}$ and $E_{\Gamma_j}^{A(B)}$ are the energy values and wave functions of the single-ion Hamiltonian $\hat{H}(l)$ ($l \in A$ and B, respectively). The latter, in turn, contains the longitudinal susceptibility $\chi_{\|}$ which, thus appears both at the right- and left-hand sides of Eq. (8).

For temperatures higher than the Néel point, the longitudinal magnetic susceptibility $\chi_{\|}^0$ goes over into the paramagnetic susceptibility. To obtain the latter, we make use of the same equation as that for $\chi_{\|}$ albeit with $\mathscr{H}_{mf}^A$ and $\mathscr{H}_{mf}^A$ put equal to zero. Having obtained

$\chi_{||}$, we return to the magnetizations and consider their dependences both on temperature in the presence of the external field and on the external magnetic field strength at different selected temperatures. To achieve this, we have recourse to Eqs (7) in which, instead of $\mathcal{H}_{\mathrm{mf}}^{A(B)}$, we insert $\mathcal{H}_{\mathrm{mf}}^{A(B)}+H_z(1+\lambda_p\chi_{||})$. Moreover, we calculate the temperature dependence of the magnetic specific heat by having recourse to the formula (cf. Part I of this paper):

$$C_{\mathrm{H}} = \tfrac{1}{2}(C_{\mathrm{H}}^{A}+C_{\mathrm{H}}^{B}). \tag{9}$$

where

$$C_{\mathrm{H}}^{A(B)} = \left(\frac{\partial\langle\hat{H}(l)\rangle}{\partial\theta}\right)_{H_z} \tag{9a}$$

and l belong to the sublattice A or B, respectively.

3. *Numerical results and their discussion*

Let us first discuss the range of variability of the parameters to which we have recourse in our considerations. We assume that the system orders antiferromagnetically at $T = 20$ K, and allow the crystal-field parameter B_4 to vary. In our numerical calcula-

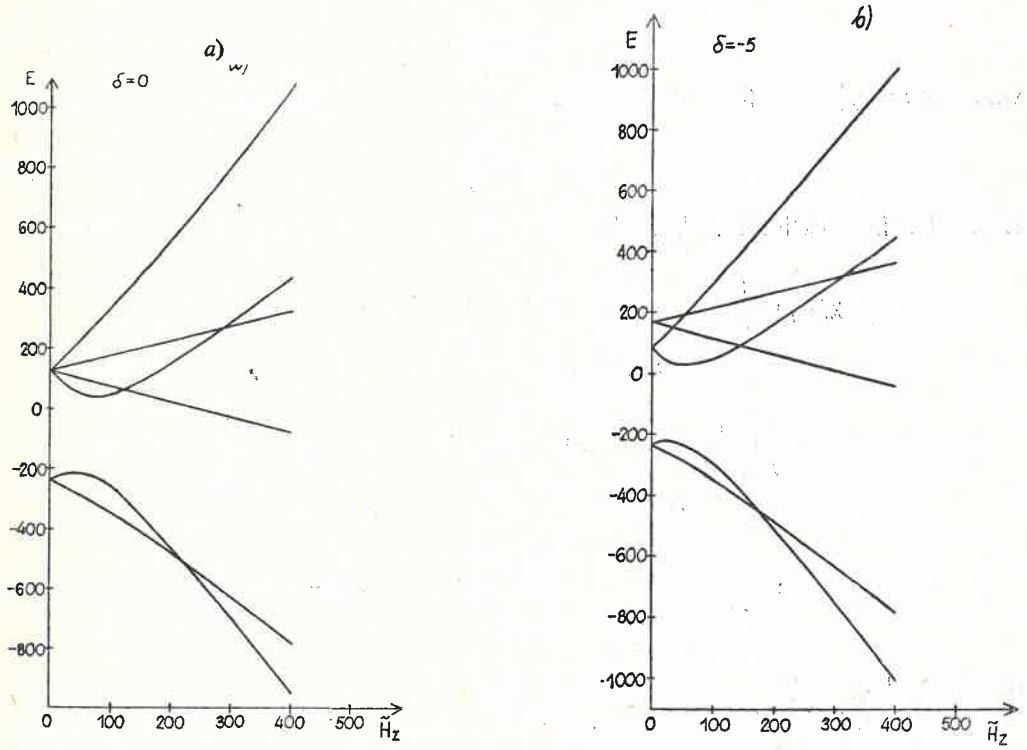

Fig. 1. The six energy levels of the Ce^{+3} ion in octahedral environment versus the magnetic field strength directed along the (001) crystal axis. The energy is expressed in units of the crystal-field parameter B_4. The magnetic field is expressed in dimensionless form: $\tilde{H}_z = g\mu_B H_z/B_4$. a) $\delta = 0$ without tetragonal distortion, b) $\delta = -5$ with the tetragonal distortion

tions B_4 took the following values: 0.02778 K, 0.05556 K, 0.08333 K and 0.16667 K. As known (see Part I of the paper), B_4 defines the energy gap between the ground-state doublet and excited crystal-field level (a quartet if $\delta = 0$ and a doublet if $\delta \neq 0$) (Figs 1a and 1b). The four selected values of B_4 correspond to crystal-field splitting comparable with the exchange, when anomalies occur in the behaviour of the magnetic observables, as was indicated previously (see, for example, [2, 3, 13, 14]). The parameter δ determining the relative magnitude of the second-order crystal-field potential is maintained constant and equal to -5 (see [12]).

The antiferromagnetic molecular-field constant λ_{af} is estimated from the inverse crystal-field-only susceptibility at $T = T_N$ (the Néel temperature) (cf. [1–3, 13, 14]).

The paramagnetic molecular-field constant λ_p can be derived from a comparison of the inverse paramagnetic susceptibility including the crystal-field effects and the usual Curie-Weiss inverse susceptibility at temperatures much higher than the crystal-field splitting between the ground and the excited energy levels. Extrapolation of the high-temperature behaviour of χ_p^{-1} yields the following expression for λ_p (see [1, 2]):

$$\lambda_p = kT_c/C_M, \tag{10}$$

where C_M is a factor including the crystal-field effects given by

$$C_M = \tfrac{1}{6} \sum_{i,j=1}^{6} |\langle \Gamma_i, J^z \Gamma_j \rangle|^2, \tag{10a}$$

where $|\Gamma_{i(j)}\rangle$ are the crystal-field eigen-states, and T_c is the paramagnetic Curie temperature. Since, in an actual crystal, T_c can be either positive, negative or zero depending on the details of the exchange interaction, in our model calculation we have put $T_c = 0$ and ± 10 K.

Let us now proceed to a discussion of our numerical results. First, we shall briefly interpret the temperature-behaviour of the selected magnetic quantities in the light of the energy structure of the Ce^{+3} ion.

Obviously, at zero external magnetic field, the sublattice magnetizations are equal to each other but have opposite signs. As an example, we have plotted the temperature variation of the sublattice A magnetization for $B_4 = 0.05556$ K and 0.16667 K with and without the tetragonal distortion. As seen, the presence of the latter does not influence the qualitative picture. For $B_4 = 0.05556$ K, the crystal-field energy gap between the ground and excited level is equal to kT_N. At low temperatures ($\lesssim 5$ K), there occurs a sharp decrease in $\langle J_A^z \rangle$ with increasing temperature [2, 3]. In order to explain this anomaly we have recourse to the Ce^{+3} ion energy structure (Fig. 1). At low temperatures the main contribution to the magnetization is contributed by the magnetic singlets arising in the crystal-field group doublet. Therefore, neglecting the contribution from the higher energy levels, we can write:

$$\langle J_A^z \rangle = \frac{\sum_{i=1}^{2} \langle \Gamma_i, J^z \Gamma_i \rangle e^{-E\Gamma i/\theta}}{\sum_{j=1}^{2} e^{-E\Gamma i/\theta}} \tag{11}$$

where E_{Γ_i} and $|\Gamma_i\rangle$ $(i = 1, 2)$ are the eigen-values and eigen-states, respectively, of the Hamiltonian $\hat{H}(l)$ $(l \in A)$ with H_z put equal to zero.

At zero temperature, the magnitude of the sublattice molecular field is larger than that for which the lower-lying singlets cross each other $(E_{\Gamma_2} < E_{\Gamma_1})$. With increasing temperature the energy gap between these singlets i. e. $E_{\Gamma_1} - E_{\Gamma_2}$ decreases until it becomes equal to zero. Let us rewrite Eq. (11) in the following form:

$$\langle \hat{J}_A^z \rangle = \frac{\langle \Gamma_1, \hat{J}^z \Gamma_1 \rangle e^{-\frac{E_{\Gamma_1} - E_{\Gamma_2}}{\theta}} + \langle \Gamma_2, \hat{J}^z \Gamma_2 \rangle}{e^{-\frac{E_{\Gamma_1} - E_{\Gamma_2}}{\theta}}}. \tag{11a}$$

As the temperature increases from zero the second magnetic singlet also becomes populated since $E_{\Gamma_1} - E_{\Gamma_2}$ is very small. Consequently, there is an increase both in the numerator and denominator of Eq. (11a). Since at low temperatures the value of $\langle \Gamma_2, \hat{J}^z \Gamma_2 \rangle$ is larger than that of $\langle \Gamma_1, \hat{J}^z \Gamma_1 \rangle$, the increase in nominator is smaller and $\langle \hat{J}_A^z \rangle$ exhibits a sharp decrease as the values of θ and $E_{\Gamma_1} - E_{\Gamma_2}$ approach each other.

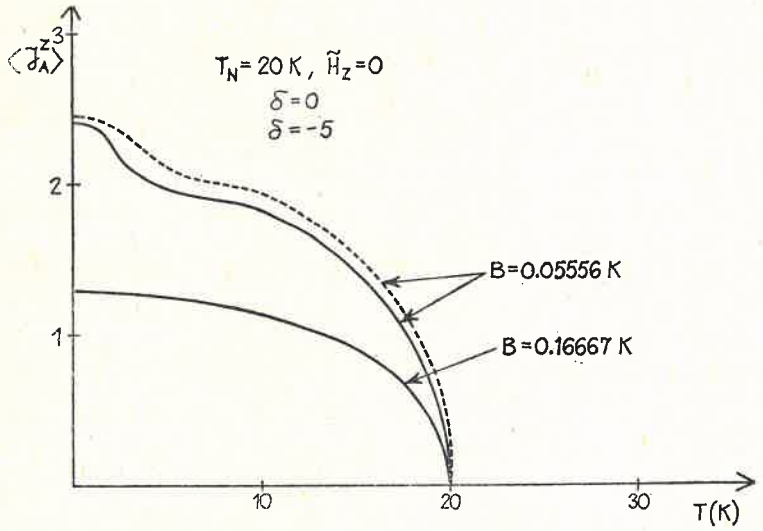

Fig. 2. Temperature-variation of the sublattice magnetization per ion, $\langle J_A^z \rangle$, for the (001) direction, $T_N = 20$ K, $B_4 = 0.05556$ and 0.16667 K, $\delta = 0$ and -5. The sublattice magnetization is expressed in units of $g\mu_B$

For larger values of B_4 the anomalies in temperature variation of $\langle \hat{J}_A^z \rangle$ vanish since the magnitudes of the sublattice molecular fields are much lower than that at which the crossing occurs (see Fig. 2, $B_4 = 0.16667$ K).

It is also of considerable interest to study the influence of the field applied along the magnetic ordering on the temperature behaviour of the sublattice magnetizations. As an illustration of our numerical calculations, we have plotted the results for $B_4 = 0.05556$ K (see Fig. 3). The anomalies derived by us for $T \leqslant 5$ K occur also. As seen, the difference

in sublattices magnetizations depends strongly on the magnitude of the applied field. The external field increases a magnitude of the moment of the sublattice A, whereas reduces a magnitude of that of the sublattice B. In Fig. 3, the part of the curve $\langle \hat{J}^z \rangle$ lying above

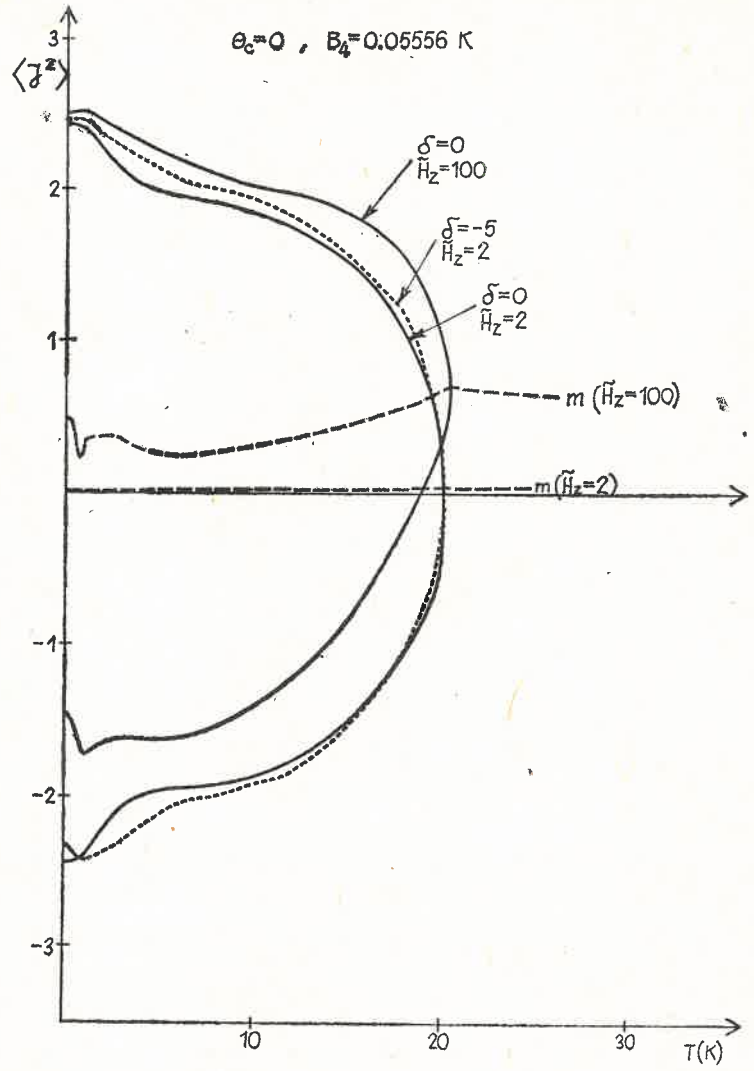

Fig. 3. Temperature-variations of the sublattice magnetizations per ion at different applied field strength $\tilde{H}_z$, for $B_4 = 0.05556$ K, $\delta = 0, -5$. The total magnetization m is also plotted

the crossing with the appropriate curve m corresponds to the sublattice A, whereas the lower part of the curve $\langle \hat{J}^z \rangle$ — to the sublattice B.

Figs. 4 and 5 show the temperature variations of the inverse longitudinal susceptibility without and with an external field. As was already discussed in Part I of the present paper, the behaviour of the susceptibility can be easily interpreted by comparing the Curie-

-Langevin and Van-Vleck type contribution (Eq. (8b)) which always exist simultaneously in systems with the Kramers degeneracy (see, for example, [1–11, 13, 14]). Contrary to the crystal-field-only case, combined crystal-field and exchange effects give rise to a strong temperature-dependence of the two contributions: directly by way of the factor $1/\theta$, and

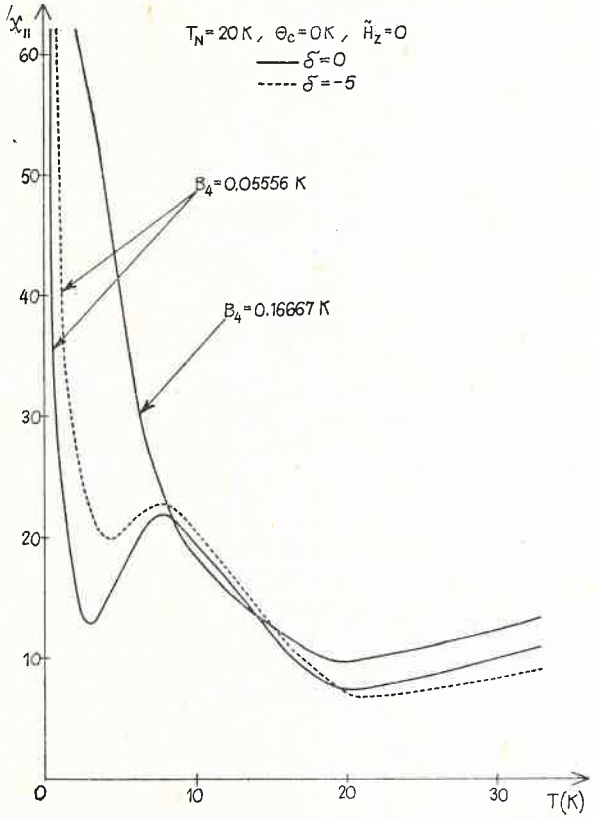

Fig. 4. Temperature-variations of the inverse longitudinal susceptibility without external field for $B_4 = 0.05556$ and 0.16667 K. The longitudinal susceptibility is expressed in units of $g^2\mu_B^2$; $\theta_c = kT_c$

indirectly by way of the molecular-field energies and the matrix elements of $\hat{J}^z$ in the molecular-field eigen-states. In the presence of an external field, there occurs a characteristic jump at the temperature of the phase transition. At temperatures higher than $T = 20$ K, the behaviour of the inverse susceptibility does not diverge essentially from that exhibited in the crystal-field-only case (cf. Part I). The Curie paramagnetic temperatures T_c, different from zero, give rise only to a shift in the inverse susceptibility curves from the appropriate crystal-field-only ones [1, 2]. It is obvious that our simplified model cannot explain all the anomalies observed in experiments on Kramers light rare-earth compounds [1–9]; moreover, many results concern polycrystalline samples for which one ought to consider also the perpendicular susceptibility, as was done, for example, by Wang and Cooper for Ce-group-V-compounds [2, 3]. However, contrary to their conclusions, we obtain here that the anomalous temperature behaviour of the inverse susceptibility

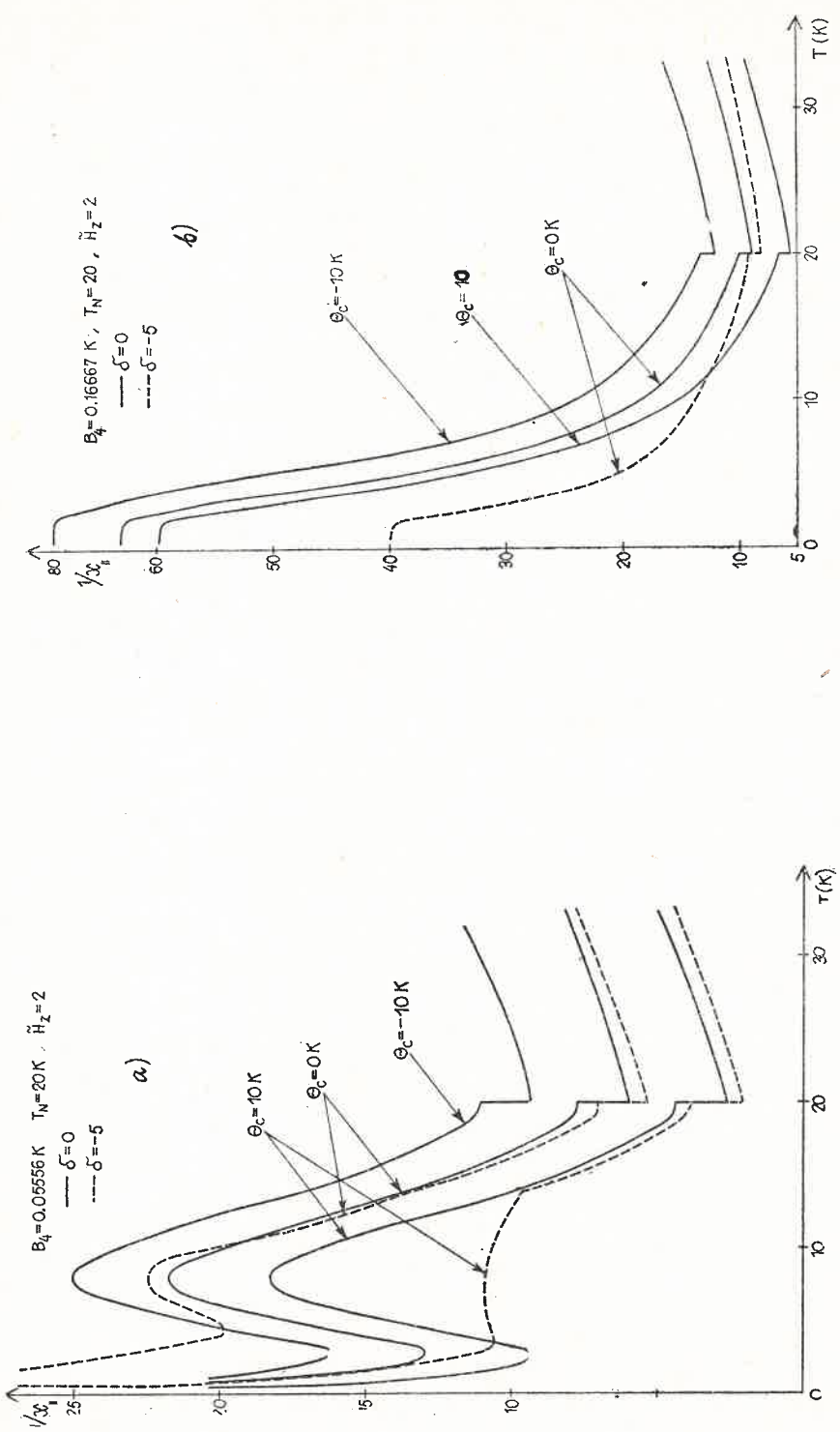

Fig. 5. Temperature-variations of the inverse longitudinal susceptibility at applied field strength $\tilde{H}_z$ equal to 2; $\theta_c = kT_c$. a) $B_4 = 0.05556$ K, b) $B_4 = 0.16667$ K

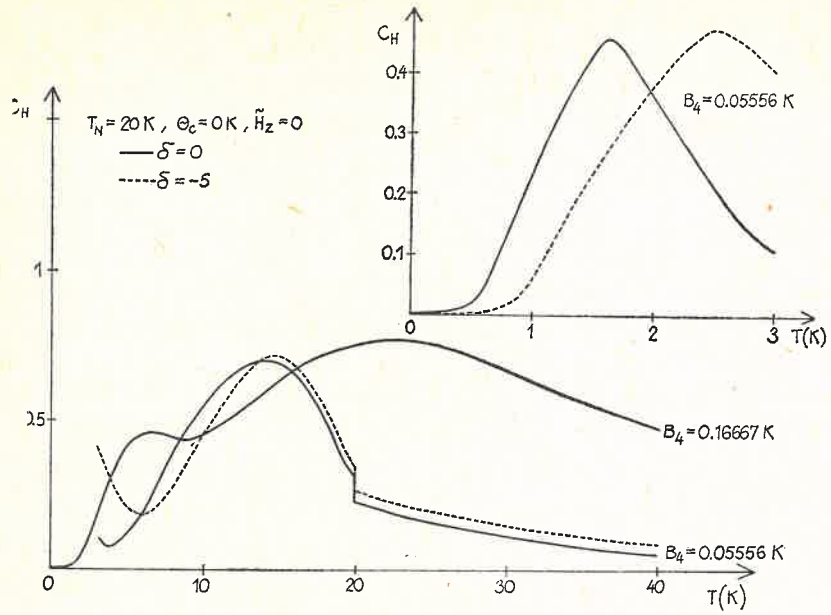

Fig. 6. Temperature-variations of the specific heat without external field for $B_4 = 0.05556$ K, $B_4 = 0.16667$ K; $\theta_c = kT_c$

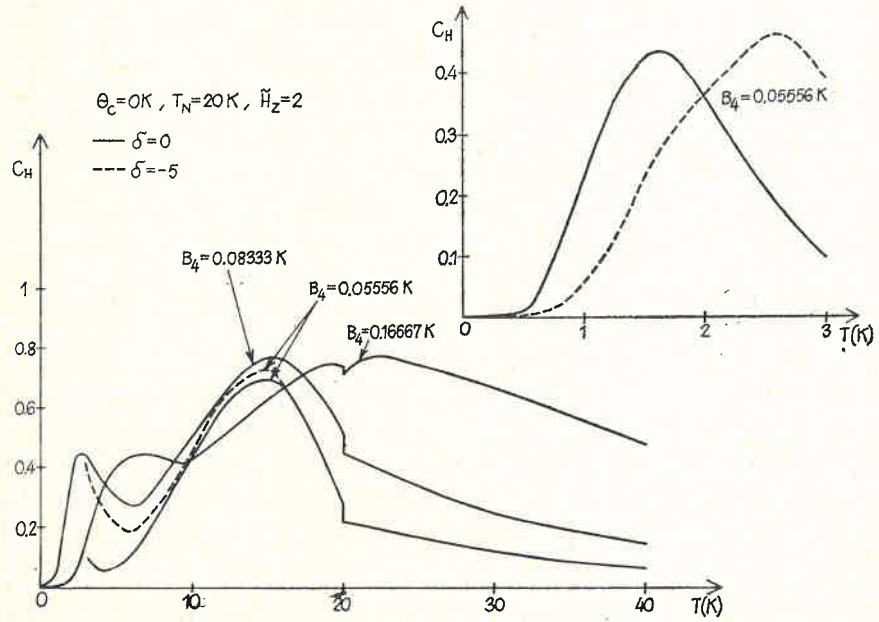

Fig. 7. Temperature-variations of the specific heat at applied field strength $\tilde{H}_z$ equal to 2; $\theta_c = kT_c$

can be attributed in part to that of the inverse longitudinal susceptibility. The anomalies obtained are particularly apparent for the case of crystal-field energy gaps nearly equal to kT_N i. e. for $B_4 = 0.05556$ K (see Figs. 4 and 5a). The anomalous broad peak occurs in the vicinity of the temperature at which the doublet levels cross each other. No such anomalies occur for $B_4 = 0.16667$ K (see Fig. 5b).

The temperature variations of the specific heat for several cases are plotted in Figs 6 and 7. The peaks depict the Schottky anomaly; there appear two peaks: the first, at low temperatures, corresponds to the splitting of the lower-lying doublet due to the molecular-field; the second, at high temperatures, is related with the energy gap between the doublet levels and those of the excited quartet or doublet. The magnetic phase transition is reflected in the temperature behaviour of C_H.

In Fig. 8 we have plotted the sublattice magnetizations per ion against the applied field strength $\tilde{H}_z = g\mu_B H_z/B_4$ at the temperature $T = 2$ K. The behaviour of the two

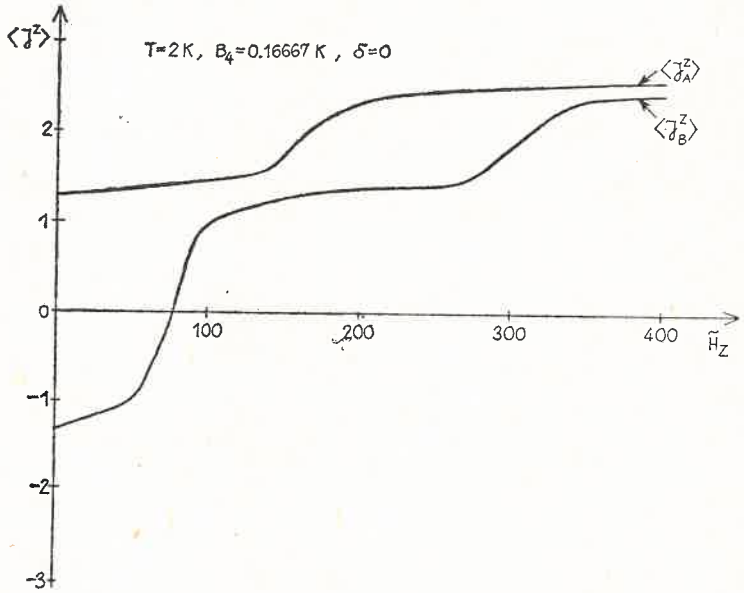

Fig. 8. The sublattice magnetizations per ion versus the magnetic field strength $\tilde{H}_z$ at temperature equal to 2K, for $B_4 = 0.16667$ K, $\delta = 0$ and $\theta_c = 0$; $\theta_c = kT_c$

magnetizations is strongly differentiated. Since the temperature is low, we can restrict our discussion to the contribution due to the magnetic singlets arising from the ground-crystal-field doublet (see Figs 1, 2). For $B_4 = 0.16667$ K, the magnitude of the molecular field at $T = 2$ K is much less than that of the field necessary for the crossing of the lowest-lying magnetic singlets. Let us write explicitly the simplified formulae for the A and B magnetizations (cf. also [13])

$$\langle J^z_{A(B)}\rangle = \frac{\langle \Gamma_{1(2)}, J^z \Gamma_{1(2)}\rangle + \langle \Gamma_{2(1)}, J^z \Gamma_{2(1)}\rangle e^{-\frac{|E_{\Gamma 2} - E_{\Gamma 1}|}{\theta}}}{1 + e^{-|E_{\Gamma 2} - E_{\Gamma 1}|/\theta}}, \qquad (12)$$

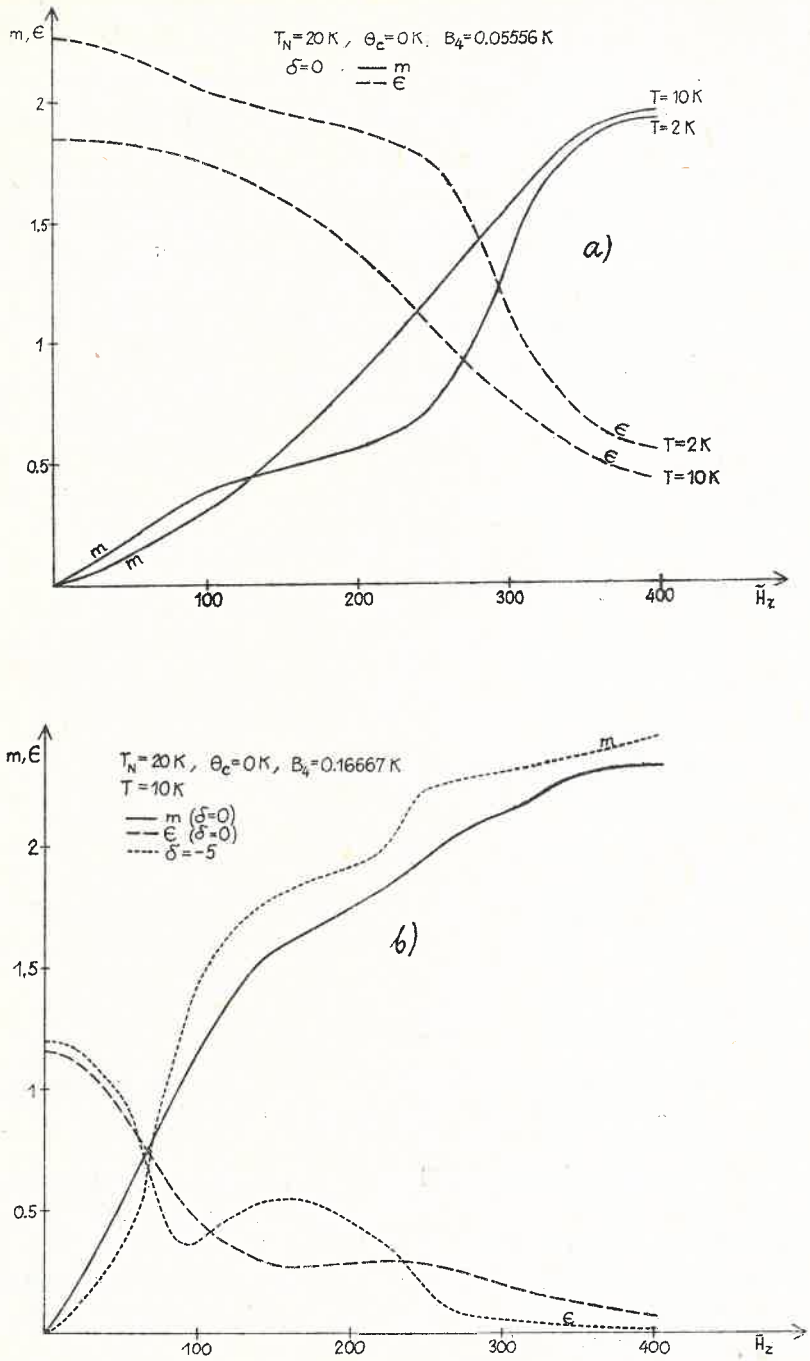

Fig. 9. The total magnetization per ion m, and the difference between the sublattice magnetizations per ion ε, versus the applied field strength $\tilde{H}_z$ at different temperatures: a) $B_4 = 0.05556$ K, b) $B_4 = 0.16667$ K; $\theta_c = kT_c$

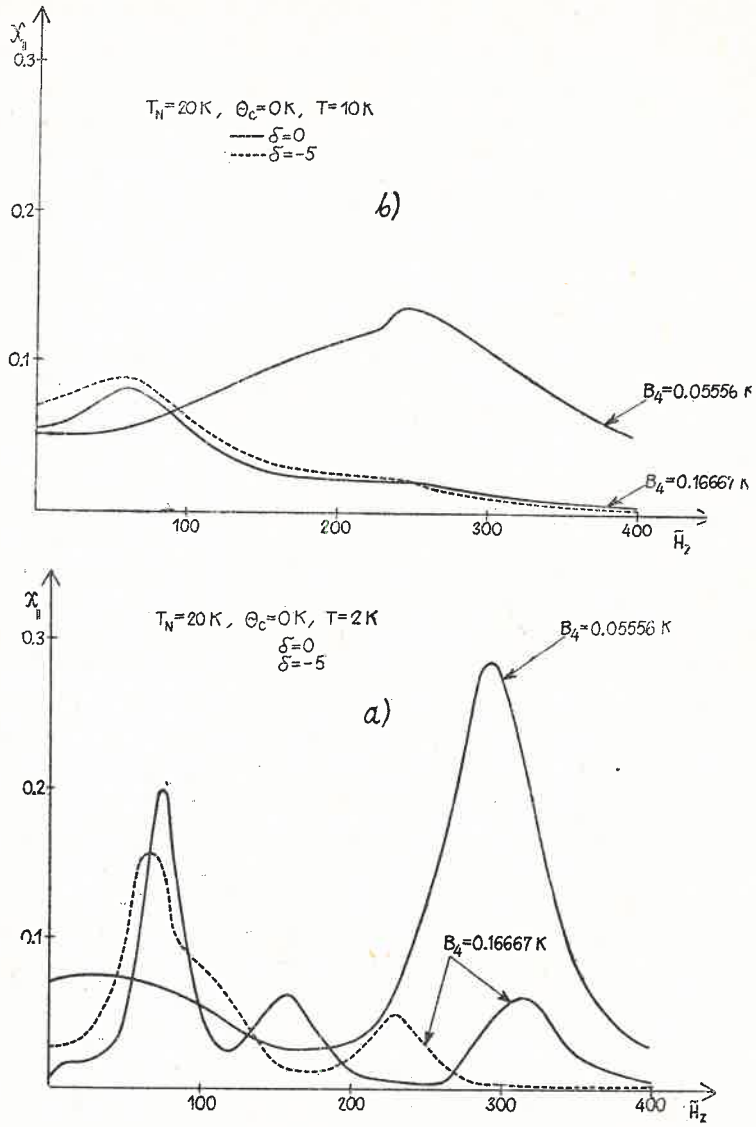

Fig. 10. The longitudinal susceptibility versus the applied field strength at different temperatures, for $B_4 = 0.05556$ K and $B_4 = 0.16667$ K; $\theta_c = kT_c$. a) $T = 2$ K, b) $T = 10$ K

where we make use of the following relations:

$$E^A_{\Gamma_1} = E^B_{\Gamma_2} = E_{\Gamma_1}; \quad E^A_{\Gamma_2} = E^B_{\Gamma_1} = E_{\Gamma_2}$$

and obviously

$$|\Gamma^A_1\rangle = |\Gamma^B_2\rangle = |\Gamma_1\rangle; \quad |\Gamma^A_2\rangle = |\Gamma^B_1\rangle = |\Gamma_2\rangle.$$

At the site A, with increasing strength of the applied field, the energy gap $|E_{\Gamma_2} - E_{\Gamma_1}|$ tends to zero. When the resultant field exceeds the strength corresponding to the crossing

of the lower-lying singlets, there occurs a sharp increase in $\langle J_A^z \rangle$, which is due to the change in ground state. Further on, $\langle J_A^z \rangle$ remains nearly constant throughout a wide range of $\tilde{H}_z$.

At a site B, the applied field is directed oppositely to the sublattice molecular field. Thus, at first, with increasing applied field, the resultant field decreases giving rise to an increase of the gap $|E_{\Gamma_2} - E_{\Gamma_1}|$ (see Figs 1, 2). $\langle J_B^z \rangle$ grows slowly until the applied field attains the value at which it cancels out with the sublattice molecular field. At zero value of the resultant field, the magnetization at a site B also vanishes and then varies slowly with increasing resultant field, albeit in the positive region. A further sharp increase corresponds to the crossing of the lower-lying singlets.

In the same way, we can interpret the diagrams shown in Figs 9a and 9b. However, one has to keep in mind that at $T = 10$ K all the energy levels of the Ce^{+3} ion have to be taken into account. We present the behaviour of the total magnetizations m and that of the difference ε between the sublattice magnetizations.

The dependence of the longitudinal susceptibility on the applied field is plotted in Figs 10a and 10b. The anomalies are more striking for lower temperatures, when the main role is played by the lowest-lying magnetic singlets. The magnitudes of the peaks as well as their positions are determined by the crystal-field parameters B_4 and δ. The occurrence of these peaks can be easily interpreted by comparing the curve for $B_4 = 0.16667$ K in Fig. 10a with Fig. 8 and also with Figs 4 in Part I of the present paper illustrating the behaviour of the crystal-field-only contribution to the susceptibility. One immediately draws the conclusion that the crystal-field effects are the most important [2, 3].

It is obvious that such a simplified model as the one proposed in our paper cannot comprise all the anomalies known from experiments on cerium compounds (see, for example, [2–10]). We have neglected information on a probable anisotropic contribution to exchange coupling, more highly complicated e. g. non-collinear magnetic structures occurring in cerium compounds [3] as well as the additional magnetic phase transitions which take place in temperatures between 0 and the Néel point. Moreover, numerous experiments have hitherto been performed only on polycrystalline samples and not monocrystals.

However, the main purpose of our paper was to study the role of the crystal field and the influence of the exchange forces on crystal field effects. To obtain a clear picture of this competition we have nonetheless chosen a model less simplified than those discussed by previous authors [1–5]. It was our intention to decide which anomalies in the magnetic behaviour can be attributed to the combined influence of the crystal field and isotropic exchange.

The behaviour of such systems at $T = 0$ K is also of great interest, as well as the conditions for their metamagnetic phase transitions. These two problems will be the subject of our next paper.

The author is strongly indebted to Professor dr hab. H. Cofta for critically reading the manuscript. Thanks are also due to Professor dr hab. L. Kowalewski for his many fruitful remarks. The numerical calculations have been performed by Mrs B. Szczepaniak, M. Sc., with an "Odra 1204" computer.

REFERENCES

[1] P. Bak, P.-A. Lindgard, *J. Phys.* **C6**, 3774 (1973).
[2] Y. L. Wang, B. R. Cooper, *Phys. Rev.* **B2**, 2607 (1970).
[3] B. R. Cooper, Lectures given at XI-th Annual Winter School for Theoretical Physics of the University of Wrocław, Karpacz 1974, Poland.
[4] T. Tsuchida, Y. Nakamura, *J. Phys. Soc. Jap.* **25**, 284 (1968).
[5] T. Tsuchida, A. Hashimoto, Y. Nakamura, *J. Phys. Soc. Jap.* **36**, 685 (1974).
[6] M. Atoji, *J. Chem. Phys.* **46**, 1891 (1967).
[7] E. Walker, H.-G. Purwins, M. Landolt, F. Hulliger, *J. Less-Common Mat.* **33**, 203 (1973).
[8] P. Schobinger-Papamantellos, P. Fisher, A. Niggli, E. Kaldis, V. Hildebrandt, *J. Phys.* **C7**, 2023 (1974).
[9] K. H. J. Buschow, J. H. N. Creyghton, *J. Chem. Phys.* **57**, 3910 (1972).
[10] B. N. Rao, Y. L. Wang, *J. Phys. Chem. Sol.* **37**, 129 (1975).
[11] P. Bidaux, A. Gavignet-Tillard, J. Hammann, *J. Phys.* **34**, 19 (1973).
[12] Cz. Rudowicz, L. Kowalewski, *Physica* **80B**, 517 (1975).
[13] P. Szweykowski, *Acta Phys. Pol.* **A51**, 549 (1977).
[14] L. Kowalewski, A. Lehmann-Szweykowska, P. Szweykowski, *J. Phys.* **C10**, 83 (1977).
[15] P. Szweykowski, *Acta Phys. Pol.* **A52**, 691 (1977).